Deuteron inelastic scattering on ^{6}Li and ^{7}Li nuclei within the three-body cluster model*

M. V. Egorov[1†] V. I. Postnikov[2]

[1]Federal State Unitary Enterprise "Russian Federal Nuclear Center" Academician E.I. Zababakhin All-Russian Research Institute of Technical Physics, Snezhinsk, Chelyabinsk Region, Russia and Physics Faculty, Tomsk State University, Lenina ave.36, Tomsk 634050, Russia
[2]National Research Nuclear University MEPhI, Moscow, Russia

Abstract: The problem of the deuteron interaction with lithium nuclei, treated as a system of two coupled pointlike clusters, is formulated to calculate the cross sections of the d+Li reaction. The d+Li reaction mechanism is described using the Faddeev theory for the three-body problem of deuteron-nucleus interaction. This theory is slightly extended for calculation of the stripping processes ^{6}Li$(d,p)^{7}$Li, ^{7}Li$(d,p)^{8}$Li, ^{6}Li$(d,n)^{7}$Be, and ^{7}Li$(d,n)^{8}$Be, as well as fragmentation reactions yielding tritium, α-particles, and continuous neutrons and protons in the initial deuteron kinetic-energy region $E_d = 0.5 - 20$ MeV. The phase shifts found for d+^{6}Li and d+^{7}Li elastic scattering, as part of the simple optic model with a complex central potential, were used to find the cross sections for the $^{6}\mathrm{Li}(d,\gamma_{M1})^{8}\mathrm{Be}$ and $^{7}\mathrm{Li}(d,\gamma_{E1})^{9}\mathrm{Be}$ radiation captures. The three-body dynamics role is also summarized to demonstrate its significant influence within the d+^{7}Li system.

Keywords: deuteron-Li, Faddeev equation, inelastic scattering, cluster model

DOI: 10.1088/1674-1137/abc248

I. INTRODUCTION

The fusion burn of Li nuclei in the $^{7}\mathrm{Li}(n,n'\alpha)t$ and $^{6}\mathrm{Li}(n,\alpha)t$ reactions under the neutrons generated at the respective facilities as a result of the $dt \to \alpha n$ controlled reaction is of importance in tritium self-reproduction. Decreased efficiency of the thermonuclear facility and malsynchronization of the tritium-reproduction cycle may be attributed to inadequate understanding of how the fast ions in preheated dt plasma interact with Li nuclei within the blanket material. Among the ion induced nuclear reactions in the thermonuclear reactor walls, the most interesting are the reactions that produce additional tritium recovery. These include the (d,t) reaction in the $^{6}\mathrm{Li}(d,t)p\alpha$, proceeding through a compound ^{5}Li nucleus, and the $^{7}\mathrm{Li}(d,t)d\ \alpha$and $^{7}\mathrm{Li}(d,t)^{6}$Li processes. An important feature of the deuteron induced reactions on Li nuclei is that they are mostly exothermal reactions, ranging from (d,γ) radiation capture to partial fragmentation of the target nucleus into three or more clusters. The energy thus removed by the deuterons from the dt reaction site may be partially compensated by additional tritium produced in the blanket as well as by virtue of the charged particles formed through several exothermic reactions possible for Linucleiuptothedeuteronkinetic-energylevel$E_d = 20$MeV.

Most experimental studies of deuteron-Li reactions were carried out in the last century. Tritium formation on the ^{6}Li and ^{7}Li isotopes in the energy region $E_d \le 4$ MeV was investigated in [1]. The angular distributions were not measured. More details were given in relation to the formation of charged particles – helium and hydrogen isotopes – in the course of the deuteron-Li reactions. Formation of two α-particles was an active area of research in [2-6]. The total cross sections of the(d, p, or n) stripping reactions, accompanied by formation of both unstable ^{7}Be [2, 7, 8] and ^{8}Li [2, 9, 10] and stable ^{7}Li [2, 3] nuclei, were measured. Currently, there are no data regarding the $^{7}\mathrm{Li}(d,n)^{8}\mathrm{Be}$ exothermal reaction. No evidence of the three-body break up reactions with the three particles being formed in the final state was given either. Such reactions refer to the above-mentioned studies [7, 8], focusing on the reactions to convert an initial scattering state into a two-neutron one. This also applies to [11], where total cross sections of the ^{6}Li $(d,n^{3}\mathrm{He})^{4}$He and ^{6}Li $(d,p^{3}\mathrm{H})^{4}$He three-body break up reactions were measured in the energy region $E_d \leqslant 0.8$ MeV. Although the d+Li system has always attracted much interest, there are no data on some of the d+Li reactions, such as $^{6}\mathrm{Li}\ (d,2d')\alpha$, $^{6}\mathrm{Li}(d,np)^{6}\mathrm{Li}$, $^{7}\mathrm{Li}(d,2\alpha)n$, $^{7}\mathrm{Li}(d,d')t\alpha$, and $^{6}\mathrm{Li}\ (d,np)^{7}\mathrm{Li}$. There are also no data on (d,γ) radiation capture for both ^{6}Li and ^{7}Li nuclei, although there is some evidence of the resonance structure in the $^{7}\mathrm{Li}\ (d,\gamma)^{9}\mathrm{Be}$ process in the en-

Received 3 July 2020; Accepted 22 September 2020; Published online 5 November 2020

* The reported study was funded by RFBR, (20-02-00004)

† E-mail: egorovphys@mail.ru

ergy region E_d = 0.35-0.4 MeV [9].

The theoretical treatment in this field primarily covers the refined optical models, with parameters selected to describe differential-angular distributions of deuteron elastic scattering by Li nuclei. The most detailed study of deuteron elastic scattering is given in Ref. [12] at E_d = 3-50 MeV and in Ref. [13] at E_d = 10-50 MeV. The latter study reports on sets of optical model parameters found for the considered energy region. They are used in calculations within the continuum discretized coupled-channels (CDCC) formalism to describe the differential cross sections of deuteron elastic scattering. The optical models used in the context of the coupled-channel formalism can provide useful information on the total contribution of various inelastic channels in their total cross sections (the so called reaction cross section), as well as on the partial cross sections, but the available references do not give such predictive calculations. There are only calculated cross sections for the inclusive ^{7}Li (d,Xn) and ^{7}Li(d,Xp) reactions to predict the total yield of continuum neutrons and continuum protons in the dipole giant-resonance energy region $E_d \geqslant 20$ MeV [14], in which the main contribution to the cross-section comes through Glauber (diffraction) scattering. In addition, there are crude estimates for the s-wave cross section of deuteron induced reactions on the ^{7}Li [15] nucleus in the energy region E_d = 0.4-1 MeV. Use of the statistical Hauser-Feshbach model with formation of a combined nucleus and its break-up, irrespective of the triggering mechanism, appears to be dubious and of limited value in Ref. [16] for a light nuclei with an open p-shell and a small number of neutron resonances. Currently, microscopic models of the deuteron-Li reactions are unavailable, and they have not yet been studied systematically. The present work focuses on addressing the lack of understanding in this area.

In this work, we consider the target nucleus as a bound two-body system. This allows us to solve the scattering problem based on the integral Faddeev equations. These equations are further used to describe the nuclear-reaction cross sections. With such an approach, we avoid searching for an efficient optical potential to describe the target nucleus. At the same time, coupling of inelastic two-body channels in the d+Li reaction is equally considered while in preparation for the seed two-body interactions. In addition, the few-body microscopic approach resolves the question concerning how this or that cluster interaction contributes to the nuclear-reaction intensity.

Chapter I briefly describes the nucleus cluster model and the three-body deuteron-Li reactions in the energy region E_d = 0.5-20 MeV. Chapter II gives classification of the most relevant deuteron-Li reactions, in terms of the input into their total cross section, along with the associated measured cross sections. The final part of the work provides a Discussion of the Results, followed by the Conclusion.

II. DEUTERON SCATTERING IN THE TARGET NUCLEUS CLUSTER MODEL

In the cluster model, the lowest-energy state of the nucleus-target is determined by pairwise interaction of the $(\alpha-d)$ clusters forming the ^{6}Li and $(\alpha-t)$ clusters forming the ^{7}Li. Thus, the cluster system is in a state wherein the quantum numbers are equivalent to the corresponding numbers of target nucleus. Let the $\vec{p}$ momentum specify motion in the coupled cluster and $\vec{q}$ characterize the motion of the spectator-particle with respect to the coupled pair. The prime over the variables corresponds to the momenta resulting from particle transfer. The $\alpha,\beta,\gamma \in (1,2,3)$ indices specify the type of particular three-body cluster state, and repetitive rearrangement of Greek indices provides a set of independent values X, characterizing the probability amplitude for transition from one cluster channel to the other. Then, the integral three-body Faddeev equations, considering the adopted notations, are as follows:

$$X_{\beta\alpha}(\vec{q}',\vec{q},E) = Z_{\beta\alpha}(\vec{q}',\vec{q},E) + \sum_{\substack{\gamma=1\\ \gamma\neq\beta}}^{3}\int \frac{\mathrm{d}^3q''}{(2\pi)^3} Z_{\beta\gamma}(\vec{q}',\vec{q}'',E) \times \tau_\gamma(\vec{q}'',E) X_{\gamma\alpha}(\vec{q}'',\vec{q},E). \quad (1)$$

In Eq. (1) $\tau_\gamma(\vec{q}'',E)$ are two-body propagators that depend on the three-body kinetic energy E. The driving terms $Z_{\beta\alpha}$ are the matrix elements of the free three-body Green's function $G_0(E)$:

$$Z_{\beta\alpha}(\vec{q}',\vec{q},E) = (1-\delta_{\beta\alpha})\langle \vec{q}',\beta \,|\, G_0(E) \,|\, \vec{q},\alpha\rangle. \quad (2)$$

Condensed index γ (as well as α,β) determines the following sets of states:

$$|\vec{q},\vec{p},\gamma\rangle_{^6\mathrm{Li}} = \begin{cases} |\, d-(d\alpha),\vec{q},\vec{p}\rangle, & \gamma=3,\\ |\, d-(d\alpha),\vec{q},\vec{p}\rangle, & \gamma=2,\\ |\, \alpha-(dd),\vec{q},\vec{p}\rangle, & \gamma=1; \end{cases}$$
$$|\vec{q},\vec{p},\gamma\rangle_{^7\mathrm{Li}} = \begin{cases} |\, d-(t\alpha),\vec{q},\vec{p}\rangle, & \gamma=3,\\ |\, t-(d\alpha),\vec{q},\vec{p}\rangle, & \gamma=2,\\ |\, \alpha-(dt),\vec{q},\vec{p}\rangle, & \gamma=1. \end{cases} \quad (3)$$

The on-shell three-body kinetic energy is determined by the two-body kinetic energy and the energy E_b of the bound state. In general, the solution technique of Eq. (1) is similar to determining the solutions in Ref. [17] and will not be used here. It will only be noted that the first two states in Eq. (3) for ^{6}Li can be combined. We will discuss the two-body cluster subsystems in more detail below.

A. Two-body interactions

Interactions in each pair of particles are specified by the following separable potentials:

$$v_\gamma^{l'l} = \lambda_\gamma^{l'l}\xi_\gamma^{l'}(p')\xi_\gamma^{l}(p), \tag{4}$$

which are transformed as tensors in the orbital (l,l') momenta space of the interacting pairs of clusters. In calculations, for the interacting pairs, we adopt the following states:

$$\begin{cases} dd-(l,J^P)=(0,0^+),(0,2^+),(1,1^-), \\ d\alpha-(l,J^P)=(0,1^+),(1,0^-),(1,1^-), \\ dt-(l,J^P)=(1,3/2^-), \\ \alpha t-(l,J^P)=(1,3/2^-). \end{cases} \tag{5}$$

From the sets in Eq. (5), it follows that for both ^{6}Li and ^{7}Li nuclei, each matrix element $X_{\beta\alpha}$ contains p-wave scattering. This suggests that the three-body matrices have a complicated spin-angular structure. It is precisely for the simplicity of calculations that we restrict ourselves to the $l,l'\in(0,1)$ requirement; furthermore, it will be demonstrated that it is quite sufficient for description of the typical cross-sectional properties in most of the considered reactions. In any two-body subsystem, for all states given in Eq. (5), the $\xi(\vec{p})$ form-factors have a similar functional form:

$$\xi(\vec{p}) = \frac{c_1}{\vec{p}^2+\beta_1^2} + \frac{c_2\vec{p}^2}{(\vec{p}^2+\beta_2^2)^2}. \tag{6}$$

$c_{1,2}$ and $\beta_{1,2}$ parameters are found from the best-description condition based on the δ_l^J phase-shift parameters and the inelasticity η_l^J (J-total spin) available in the literature. Additionally, it should be noted that in this work, in all the cluster states, the $\lambda_\gamma^{l'l}$ interaction intensity is independent of the energy. The two-body T-matrix with respect to the inelastic channels up to the order of smallness with respect to λ intensity takes the following form:

$$\begin{aligned} T(p,p') &= \xi(p)\tau(p,p^2/2\mu)\xi(p'); \\ \tau(p,p^2/2\mu) &= (\lambda^{-1}-\Sigma_{\rm el}(p)-\Sigma_{\rm inel}(p))^{-1}, \end{aligned} \tag{7}$$

wherein the energy shifts $\Sigma_{\rm el/inel}$ in the propagator are calculated using the form-factors in Eq. (6),

$$\begin{aligned} \Sigma_{\rm el}(p) &= \frac{\mu}{\pi^2}\int_0^\infty \frac{p'^2{\rm d}p'\xi^2(p')}{p^2-p'^2+{\rm i}\varepsilon}, \\ \Sigma_{\rm inel}(p) &= \frac{\mu}{\pi^2}\int_0^\infty \frac{p'^2{\rm d}p'\xi_{\rm inel}^2(p')}{p^2-p'^2+{\rm i}\varepsilon}, \\ \xi_{\rm inel}(p') &= \frac{c_3}{\vec{p}^{\,2}+\beta_3^2}. \end{aligned} \tag{8}$$

Quantity $\Sigma_{\rm inel}$, like form-factors $\xi_{\rm inel}$, is introduced to take into account some inelastic effects that are important in elastic nucleus-nucleus scattering. There is no doubt that this inclusion should be in coincidence with rearrangement matrix elements $X_{\beta\alpha}$. In this case, the eigenstate of the initial nucleus is a vector strained on elastic as well as rearrangement channels. In this work, for the sake of simplicity, we avoid direct inclusion of all of the rearrangement channels in the matrix $X_{\beta\alpha}$, retaining only the energy shift in two-body propagators.

For the αd and αt bound states with the E_b binding energy, the interaction intensity is found according to the formula

$$\lambda^{-1} = \frac{\mu}{\pi^2}\int_0^\infty \frac{(\xi^2(p)+\xi_{\rm inel}^2))p^2{\rm d}p}{(2\mu\mid E_b\mid +p^2)}. \tag{9}$$

Figure 1 shows results of the phase-shift parametrization, as well as the inelasticity parameters for dd and $d\alpha$ scattering. For dt elastic scattering, the data on the phase shifts in the pertinent energy region are unavailable. Instead, we will rely on the fact that this interaction in the considered energy region is characterized by high inelasticity related to a neutron source reaction $dt\to\alpha n$. The η inelasticity parameter characterizes the reaction cross section σ_r in the specified spin-orbital state (for the purpose of simplification, the corresponding indexes are omitted).

$$\sigma_r = \frac{\pi}{k^2}\sum_{l=0}^{\infty}(2l+1)(1-\eta^2). \tag{10}$$

Here, k is a wave-number of the relative motion vector for the d and t nuclei. Then, using the parametrized differential cross section $\sigma(\theta)$ of the neutron-source reaction reported in Ref. [20], we numerically integrate it for each l over the solid angle. The obtained partial cross sections of the reaction are substituted into equation (10) to express the inelasticity parameter η in the specified spin-orbital state. Figure 2 shows the inelasticity parameter η obtained in this manner for the dt interaction. Comparison to the data in Ref. [21] regarding the real part of the phase shift $\Re{\rm e}\delta_1^{3/2}$ for αt elastic scattering is also presented here. Table 1 summarizes the two-body cluster interaction parameters.

B. *d*+Li elastic scattering

In the notations adopted in Eq. (3), the T-matrix of elastic scattering corresponds to X_{33}, and the matrix associated with the partial amplitude $F^L(q)$ of the elastic scattering is

$$F^L(q) = -\frac{\mu_{d{\rm Li}}}{2\pi}NX_{33}^L(q,q,E). \tag{11}$$

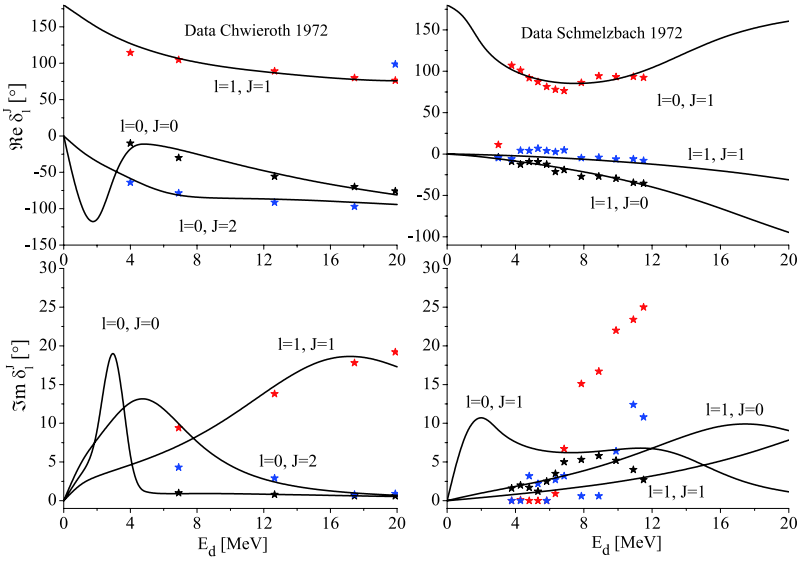

Fig. 1. (color online) Real $\Re\mathrm{e}(\delta_l^J)$ and imaginary $\Im\mathrm{m}(\delta_l^J)$ parts of phase shifts for dd scattering; data taken from [18] on the left. Real $\Re\mathrm{e}(\delta_l^J)$ and imaginary $\Im\mathrm{m}(\delta_l^J)$ parts of phase shifts for $d\alpha$ scattering; data taken from [19] on the right.

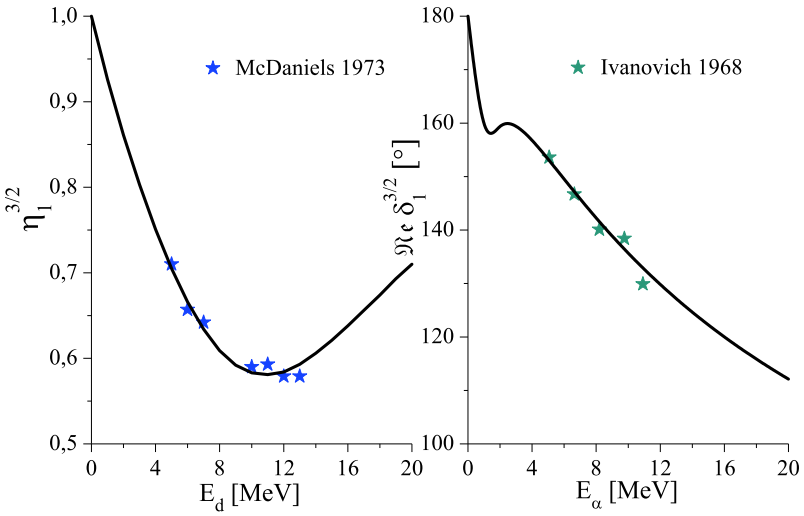

Fig. 2. (color online) Inelasticity parameter $\eta_1^{3/2}$ for dt scattering; the results are based on [20] (see in the text) on the left. Real part of $\delta_1^{3/2}$ phase shift for αt scattering; data taken from [21] on the right.

Table 1. Intensity λ of the two-body interactions and c,β parameters that appear in the form-factors (6) and (8). In the third column, the equation number is given in parentheses.

Sys.	(l,J^P)	λ^{-1}/MeV^{-1}	c_1/MeV^2	c_2/MeV^2	c_3/MeV^2	β_1/MeV	β_2/MeV	β_3/MeV
dd	$(0,0^+)$	$-0.3\cdot 2\pi^2$	−430	345	$49/\lambda$	106	57	1
	$(0,2^+)$	$-7.75\cdot 2\pi^2$	−991	319	$14/\lambda$	300	101	5
	$(1,1^-)$	$-1\cdot 2\pi^2$	−989	588	$75/\lambda$	350	156	3.6
$d\alpha$	$(0,1^+)$	(12)	−310	320	$82/\lambda$	140	64	24
	$(1,0^-)$	$-40\cdot 2\pi^2$	−500	0	$245/\lambda$	225	–	10
	$(1,1^-)$	$-25\cdot 2\pi^2$	−989	2	$560/\lambda$	490	100	17
dt	$(1,\frac{3}{2}^-)$	$-3\cdot 2\pi^2$	−745	0	$112/\lambda$	674	–	30
αt	$(1,\frac{3}{2}^-)$	(12)	−435	100	–	169	53	–

Here, the reduced mass of the deuteron-Li is denoted by $\mu_{d\mathrm{Li}}$, where N is a normalization factor calculated from the binding energy of the cluster E_b [17]. Figure 3 shows the measured cross sections of d^6Li and d^7Li elastic scattering. The presence of resonance-like structures in the regions $E_d \approx 4$ MeV and $E_d \approx 5$ MeV is to be noted. In this paper, their formation mechanism will not be discussed in detail. The only thing to be noted here is that the full information about all the inelastic processes, possible within the adopted cluster scheme, Eq. (3), within the used parametrization, Eq. (6), has already been entered in the X_{13}, X_{23}, and X_{12} matrices, against which the matrix X_{33} is expressed. Taking into account the fact that there are no experimental data regarding d+Li elastic scattering, the major criterion for accurate prediction is agreement with the other model approximations, specifically, with the optical-model predictions. We have found that the calibrated optical predictions based on the available differential distributions are in reasonable agreement with the data in Fig. 3 for the elastic-scattering cross sections on the level of 800-900 mb in the region $E_d \geqslant 8$ MeV.

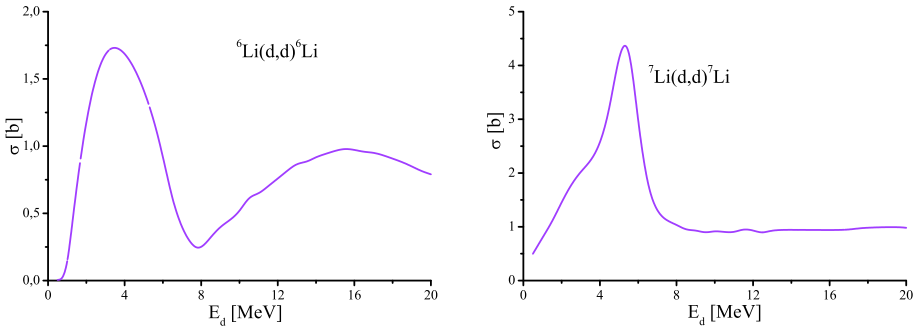

Fig. 3. (color online) Deuteron elastic scattering on the ^{6}Li (on the left) and ^{7}Li (on the right) nuclei.

III. DEUTERON-LI REACTIONS

Among the considered deuteron-Li reactions in the energy region E_d = 0.5-20 MeV, the most significant are listed below:

$$
d+{}^{6}\mathrm{Li}\rightarrow\begin{cases}\gamma+{}^{8}\mathrm{Be},\ Q=22.279,\\ 2\alpha,\ Q=22.37,\\ p+{}^{7}\mathrm{Li},\ Q=5.026,\\ n+{}^{7}\mathrm{Be},\ Q=3.382,\\ n+p+{}^{6}\mathrm{Li},\ Q=-2.224,\ E_{\mathrm{th}}=2.969,\\ 2d'+\alpha,\ Q=-1.473,\ E_{\mathrm{th}}=1.967,\\ t+p+\alpha,\ Q=2.559,\\ {}^{3}\mathrm{He}+n+\alpha,\ Q=1.7951;\end{cases}
$$

$$
d+{}^{7}\mathrm{Li}\rightarrow\begin{cases}\gamma+{}^{9}\mathrm{Be},\ Q=8.623,\\ t+{}^{6}\mathrm{Li},\ Q=-0.994,\ E_{\mathrm{th}}=1.279,\\ p+{}^{8}\mathrm{Li},\ Q=-0.192,\ E_{\mathrm{th}}=0.247,\\ n+{}^{8}\mathrm{Be},\ Q=15.029,\\ n+p+{}^{7}\mathrm{Li},\ Q=-2.224,\ E_{\mathrm{th}}=2.863,\\ \alpha+d+t,\ Q=-2.467,\ E_{\mathrm{th}}=3.176,\\ 2n+{}^{7}\mathrm{Be},\ Q=-3.869,\ E_{\mathrm{th}}=4.979,\\ 2\alpha+n,\ Q=15.121.\end{cases}
\tag{12}
$$

The masses of all nuclei were calculated using the recent values of their mass excess from [22]. In Eq. (12), the reaction energy Q and the threshold energy E_{th} are given in MeV, respectively. The amount of exothermic reactions, which (as mentioned in the introduction) might have a significant effect on the energy balance of advanced fusion facilities, is to be noted. The cross sections σ of the stripping reactions associated with the so called "two by two" reaction are expressed using the formula

$$
\frac{\mathrm{d}\sigma}{\mathrm{d}\Omega_c}=\frac{E_f E_{\mathrm{Li}}\omega_d\omega_c}{(2\pi W)^2}\frac{p_f}{p_i}\frac{1}{3(2J_{\mathrm{Li}}+1)}\times\sum_{M_i M_f}\left|\sum_{\gamma}\xi_{\gamma}(p)X_{\gamma 3}(p_i,p_f,E)N\right|^2. \tag{13}
$$

Here, W is the total system energy; ω_d and ω_c are the deuteron and light particle energy reaction product, respectively; E_{Li} and E_f are the Li-nucleus and heavy particle energy reaction product, respectively; and p_i, p_f, and Ω_c are the relative momenta of the particles before and after the reaction, as well as the solid angle of escape of light particles, respectively.

Summation in Eq. (13) is taken over the complete-spin (spin-channel) projections of the initial and final nuclear system. Index γ runs over the values [1, 2], and for the given stripping or rearrangement reaction, these values give the required final state. $\xi_{\gamma}(p)$ is an additional vertex form-factor (where $\vec{p}$ is the relative momentum of the neutron or proton and the removal particle; see Fig. 4) used in calculation of the stripping processes. Stripping

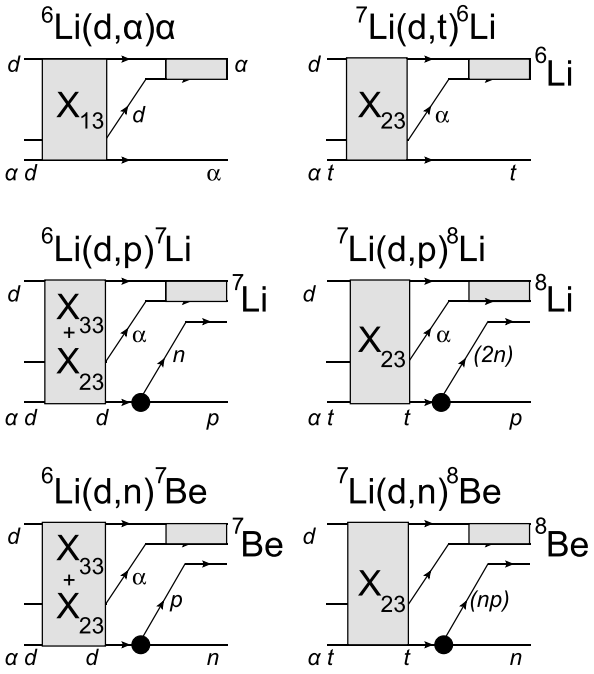

Fig. 4. Diagrammatic representation of rearrangement and stripping processes. Solid circles correspond to an additional vertex form-factor $\xi_\gamma(p)$ used in stripping processes. Propagators τ are denoted by shaded boxes. Indexing for probability amplitudes X is determined by (3).

processes, for example, ^{7}Li(d,n)^{8}Be or ^{6}Li(d,p)^{7}Li, seem to be two-step processes under the three-body approach, where the deuteron is split off on the first step and the final nucleus is formatted on the second one. Moreover, integration over the relative momentum of splitting particles is required. Instead of avoiding the inevitable numerical complexity, we neglect the propagation of splitting particles (proton, neutron, deuteron, and two neutron quasi-particle – 2n) in the nuclear medium that takes place in the stripping processes. For the stripping reactions with formation of short-lived or stable nuclei, it is typical that the interaction of the incident particle with the target nucleus seems to be of a pole type (see Fig. 4), where the pole takes the role of reduced width for only the removal proton for ^{6}Li(d,p)^{7}Li and ^{7}Li(d,p)^{8}Li or only the removal neutron for ^{6}Li(d,n)^{7}Be and ^{7}Li(d,n)^{8}Be. In this paper, for the stripping reactions, we actually use just two types of vertices. The first one is the (pn) vertex, wherein the interaction is specified by the simple rank-one separable potential [23], and the second is the (nd) vertex, achieved on the separable rank one potential with the parameters for the $1/2^+$ state [17]. Here, we do not distinguish either nd or $p(2n)$ interactions, where ($2n$) is the quasi-bound two neutron state. In this simplification, the integration over relative momentum of splitting particles is replaced by the vertex form-factor $\xi_\gamma(p)$ multiplier calculated at the mass shell relative momentum $\vec{p}$. Another simplification has been made for the three-body nature of the residual nuclei ^{7}Li, ^{8}Li, ^{7}Be, and ^{8}Be that underlies the present stripping process calculations and should be carefully taken into account in searching for bound energies. However, we avoid the direct solution of three-body problems for n-α-d, ($2n$)-α-d, p-α-d and (np)-α-d interactions in the final states and relate them to the internal structures of residual nuclei ^{7}Li, ^{8}Li, ^{7}Be, and ^{8}Be. Instead of precise calculation of the three-body final states in stripping processes, we have made an attempt to reproduce stripping cross sections from a kinematic point of view, in which we explicitly have a phase space for the reactions ^{6}Li(d,p)^{7}Li, ^{7}Li(d,p)^{8}Li, ^{6}Li(d,n)^{7}Be, and ^{7}Li(d,n)^{8}Be with residual nuclei ^{7}Li, ^{8}Li, ^{7}Be, and ^{8}Be and emitted protons or neutrons.

It should be emphasized that some information about stripping processes is already partially contained in the Σ_{inel} quantities. These terms must be in coincidence with elastic nd, np, and dt scattering data needed for $\xi_\gamma(p)$ search. Here, for the sake of simplicity, we restrict calculations by independent searching of Σ_{inel} and nd, np, and dt two-body form-factors. The amplitudes for elastic pn and nd scattering are taken into account with the use of separable rank one potentials from [23] and [17], respectively. For the dt potential, as previously mentioned, we fitted an inelastic parameter η under the separable rank one approximation. Figures 5-7 show calculated total cross sections of the considered rearrangement and strip-

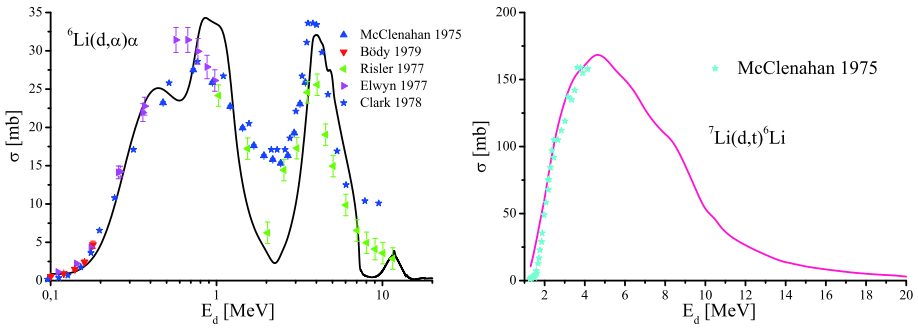

Fig. 5. (color online) Total cross sections of the ^{6}Li(d,α)α (on the left) and ^{7}Li(d,t)^{6}Li (on the right) reactions. The experimental points are from [2-6].

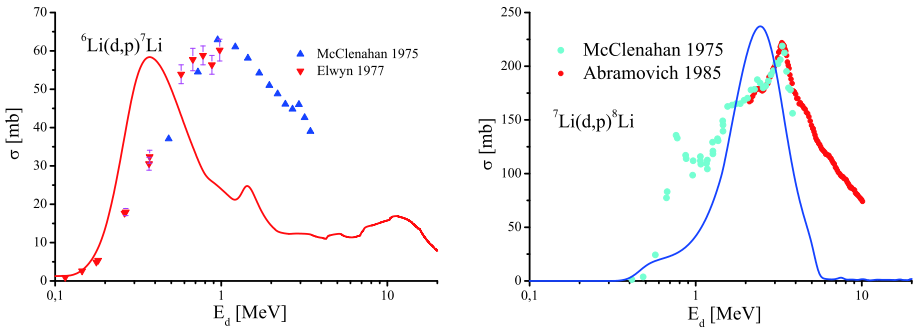

Fig. 6. (color online) Total cross sections for the ^{6}Li(d,p)^{7}Li (on the left) and ^{7}Li(d,p)^{8}Li (on the right) reactions. The experimental points are from [2, 3, 24].

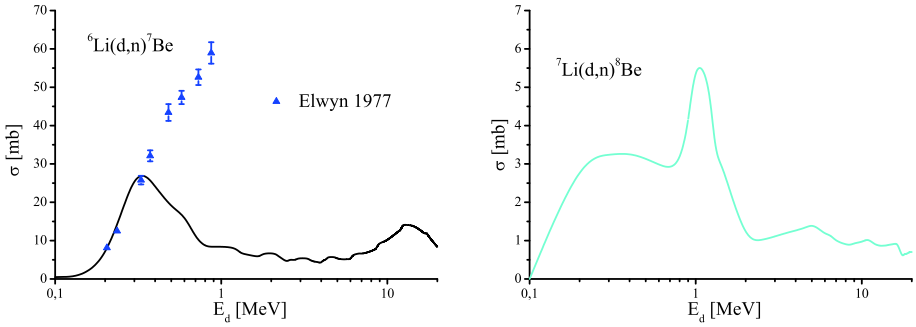

Fig. 7. (color online) Total cross sections for the ^{6}Li(d,n)^{7}Be (on the left) and ^{7}Li(d,n)^{8}Be (on the right) reactions. The experimental points are taken from [3].

ping reactions.

A. Three-body break up reactions

Within the considered energy region, the deuteron-induced reactions may have up to 4 different channels with the three particles in the final state on both stable Li isotopes. In this regard, the measured cross sections, which are not provided with the experimental data, are of interest. First of all, this applies to the reactions yielding the following sets of particles: $n+p+^{6}\mathrm{Li}$, $2d'+\alpha$, $2\alpha+n$, $n+p+^{7}\mathrm{Li}$, and $\alpha+d+t$.

The total cross section of the three-particle break up reaction is calculated via integration over the following expression:

$$\frac{\mathrm{d}\sigma}{\mathrm{d}\Omega_c d\omega_{12}\mathrm{d}\Omega_{12}} = (2\pi)^{-5}\frac{\omega_{\mathrm{d}}E_{\mathrm{Li}}\omega_c p_c E_1 E_2 p_{12}}{p_i W^2}\frac{1}{3(2J_{\mathrm{Li}}+1)} \times \sum_{M_i M_f}\Big|\sum_{\gamma=1,2,3}\tau_\gamma(\vec{p}_\gamma, E-\vec{p}_\gamma^{\,2}/2M_\gamma) \times \xi_\gamma(p_\gamma)X_{\gamma 3}(p_i,p_c,E)N\Big|^2. \quad (14)$$

New notations are introduced in Eq. (14) as compared with Eq. (13): ω_c, p_c, and Ω_c are the energy, momentum, and solid angle for one of the three escaping particles; p_{12} and Ω_{12} are the relative momentum for the other pair of particles and its solid angle calculated in the center-of-mass system of the pair, respectively; E_1 and E_2 are the energies of the other two particles in the common center-of-mass system.

Figure 8 shows calculated cross sections for the three-body break up reaction based on Eq. (14).

B. Radiation capture

The radiation-capture processes in the form

$$d(\omega_i,\vec{q}_i)+\mathrm{Li}(E_i,-\vec{q}_i)\to\gamma(\omega_\gamma,\vec{k}_\gamma)+\mathrm{Be}(E_f,\vec{p}_f) \quad (15)$$

reveal information about the internal structure of the Be nucleus and relate to the electromagnetic transitions between the excited discrete levels of the Be nucleus and low-lying or ground states. The cross section of the process given in Eq. (15) is expressed by the formula

$$\frac{\mathrm{d}\sigma}{\mathrm{d}\Omega_\gamma} = \frac{E_i E_f \omega_i \omega_\gamma^2}{q_i(2\pi W)^2}\frac{1}{3(2J_{\mathrm{Li}}+1)}\sum_{l\mu,\mathrm{EM}}\left|T_{\mathrm{BeLi}}(l\mu,\mathrm{EM})\right|^2. \quad (16)$$

In the longwave approximation, when the wave number of radiation k_γ is much smaller than the spatial dimensions of the system R, i.e., $k_\gamma\cdot R\ll 1$, that for the special case $\omega_\gamma=10$ MeV and $R=2.5$ fm yields $0.13\ll 1$, and the probability $T_{\mathrm{BeLi}}(l\mu,\mathrm{EM})$ of the electromagnetic transition of the $\mathrm{EM}\in(\mathrm{E},\mathrm{M})$ type with multipolarity $l\mu$ may be represented [25] by the following:

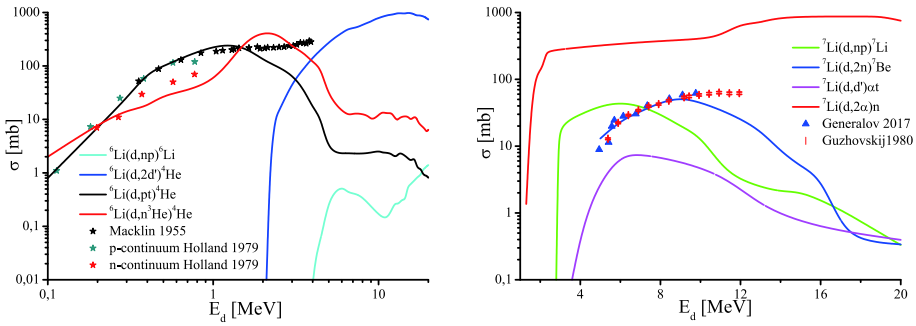

Fig. 8. (color online) Cross section of the three-body break up reaction on the ^{6}Li (on the left) and the ^{7}Li nucleus (on the right). Experimental results for the ^{6}Li(d,pt)^{4}He and ^{6}Li(d,n^3He)^{4}He reactions are in [11]; data for the ^{7}Li(d,2n)^{7}Be process are taken from [7, 8].

$$T_{\mathrm{BeLi}}(l\mu,\mathrm{EM}) = \frac{8\pi(l+1)k_\gamma^{2l+1}}{l((2l+1)!!)^2}\left|\langle \mathrm{Be}\,|\,\Omega_{l\mu}(\mathrm{EM})\,|\,\mathrm{Li}\rangle\right|^2, \quad (17)$$

where

$$\Omega_{l\mu}(\mathrm{E}) = \sum_{j=1}^{A}\Big[e_j r_j^l Y_{l\mu}(\hat{r}_j) - \mathrm{i}\frac{e\hbar c}{M_N c^2}K_j\frac{k_\gamma}{l+1}(\vec{\sigma}_j\times\vec{r}_j) \times\vec{\nabla}_j(r_j^l Y_{l\mu}(\hat{r}_j))\Big],$$

$$\Omega_{l\mu}(\mathrm{M}) = \mathrm{i}\sum_{j=1}^{A}\Big[\Big(\frac{e_j\hbar c}{2M_N c^2}\frac{2}{l+1}\vec{L}_j + \frac{e\hbar c}{2M_N c^2}K_j\vec{\sigma}_j\Big) \times\vec{\nabla}_j(r_j^l Y_{l\mu}(\hat{r}_j))\Big]. \quad (18)$$

In Eq. (18), e and e_j are the elementary charges, and $e_j = e$ for protons and $e_j = 0$ for neutrons; r_j and K_j are the coordinate of the j-th nucleon and its magnetic moment, respectively; $\vec{\sigma}_j$, $\vec{L}_j$, and $\vec{\nabla}$ are spin operators of the orbital moment and gradient acting upon the j-th nucleon.

Typically, radiation captures are calculated with complicated cluster systems. Each of them consists of several protons and neutrons. Therefore, it is advantageous to limit summation over j entirely by the initial nuclei with the effective charge ε_l. Then, for the process given in Eq. (15), the effective charge is

$$\varepsilon_l = \Big(\frac{A}{A+2}\Big)^l + 3\Big(-\frac{2}{2+A}\Big)^l. \quad (19)$$

Here, A is the atomic number of the Li nucleus. Further summation of Eq. (18) over magnetic quantum numbers with the Wigner-Eckart formula and integration over $\hat{r}_j$ angles with the $d-$Wigner function are rather time-consuming and can be found elsewhere. We will dwell on calculations of the $\langle \mathrm{Be}\,|\,r^l\,|\,\mathrm{Li}\rangle$ and $\langle \mathrm{Be}\,|\,r^{l-1}\,|\,\mathrm{Li}\rangle$ radial integrals included in Eq. (17). The d+Li scattering states are roughly approximated by the s-wave only. Then, numerically solving the Schrödinger equation with the central complex potential taking into consideration the Coulomb potential screening at r = 1.5 fm yields the appropriate radial wave functions. For the central complex potential given below,

$$\frac{V+\mathrm{i}W}{1+\exp\Big(\frac{r-r_0}{a}\Big)}, \quad (20)$$

the free parameters – the depths of the real and imaginary parts V [MeV] and W [MeV] of the potential, as well as its diffuseness a [fm] and the cutoff parameter r_0 [fm], were adjusted based on reproduction of the previously-found phase shifts and inelasticity parameter for d+Li elastic scattering using Equation (11). Figure 9 demonstrates the phase shifts as compared with the inelasticity parameters for the s-wave scattering calculated using the Faddeev equations and the optical model with the central potential given in Eq. (20). The potential parameters were taken to be equal to V = 70(^{6}Li), 30(^{7}Li), W = 30(^{6}Li), 5(^{7}Li), a = 0.15(^{6}Li), 0.1(^{7}Li), and r_0 = 1.5(^{6}Li, ^{7}Li). Figure 10 shows the calculated cross sections of the radiation captures for the transition $1^+ \to 0^+$ within the process ^{6}Li(d,γ_{M1})^{8}Be, and $\frac{1}{2}^+ \to \frac{3}{2}^-$ within the process ^{7}Li(d,γ_{E1})^{7}Be.

IV. DISCUSSION OF THE RESULTS

Structurally, the Faddeev Eq. (1) allows one to consider multiple scattering within the three-body systems. The system of Eq. (1) solved with respect to the X_{33} elastic scattering matrix can be written in the following form,

$$X_{33}(\vec{q}',\vec{q},E) = K_{31}(\vec{q}',\vec{q}'',E)X_{13}(\vec{q}'',\vec{q},E) + K_{32}(\vec{q}',\vec{q}'',E)X_{23}(\vec{q}'',\vec{q},E), \quad (21)$$

where K_{31} and K_{32} are kernels of the integral Eq. (1). Information on inelastic interactions accompanied by transfer of the clusters from one interacting pair of particles to

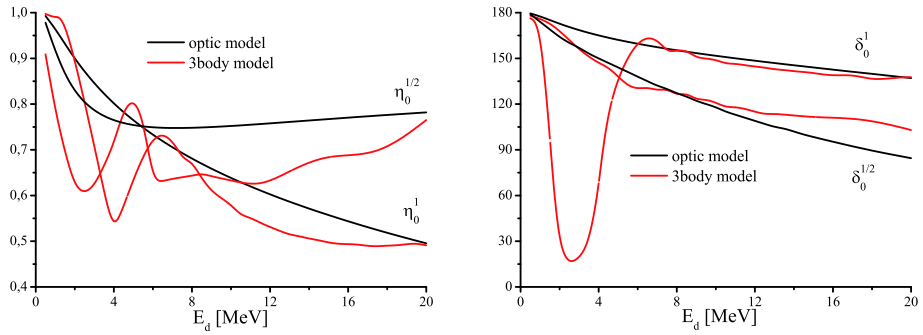

Fig. 9. (color online) Results of calculations based on the simple optical model (black lines) and exact calculation (red lines) of the inelasticity parameters (on the left) and the phase shifts (on the right) in degrees. Data on d+^{6}Li elastic scattering of η_0^1, δ_0^1 and on the d+^{7}Li elastic scattering of the $\eta_0^{1/2}$, $\delta_0^{1/2}$ are plotted.

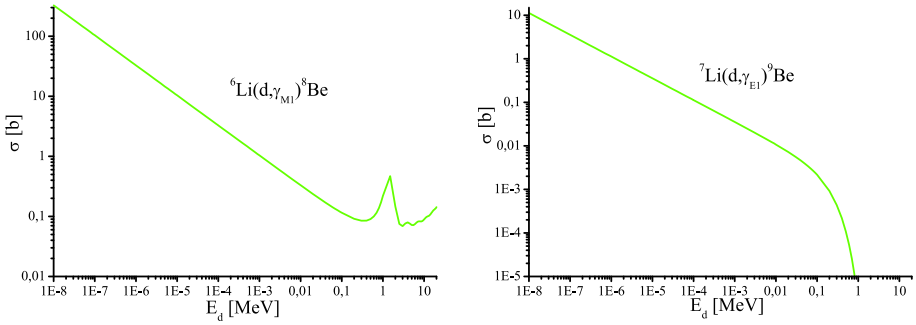

Fig. 10. (color online) Cross sections of the $^{6}\mathrm{Li}(d,\gamma_{M1})^{8}\mathrm{Be}$ (on the left) and the $^{7}\mathrm{Li}(d,\gamma_{E1})^{9}\mathrm{Be}$ radiation captures (on the right).

the other has already been added to the structure of Eq. (21). Therefore, the Faddeev equations offer an advantage in describing the processes accompanied by transformation because the amplitude obtained while constructing the elastic cross section already contains the required information for the potential inelastic processes within the system. However, the Faddeev equations cannot be simply used until, in each partial wave, the interparticle interactions are successfully parametrized, and the potentials of pairwise interactions have to reveal all the dynamic properties typical for the processes under consideration. If parametrization of the two-particle interactions is a success and the number of these interactions approaches an actual value, the chance to reach the correctly described three-particle dynamics in the considered system increases. For the same reason, we believe that if the parametrization of two-body interactions of charged particles is a success without the introduction of the Coulomb penetration factor introduction, the Coulomb forces have been indirectly taken into account.

In this work, not all of the pairwise interactions are parametrized by the phase shifts. For dt interactions, the inelasticity parameters calculated with respect to the measured cross sections for the $dt \to \alpha n$ reaction [20] were used. Our predictions show that the form of the ξ_{dt} form-factor determines the typical behavior of the elastic scattering in the region $E_d < 5$ MeV. That is why the role of this interaction has been crucial for all the reactions within the $d+^{7}$Li. At the same time, Fig. 5 shows that the cross section of the $^{7}\mathrm{Li}(d,t)^{6}\mathrm{Li}$ reaction reproduces itself quite well in the region $E_d < 5$ MeV, which suggests that the adopted functional relationship of the ξ_{dt} form-factor is quite comparable with the real one. Figures 6 and 7 show that although calculations of the stripping reaction cross sections have been considerably simplified, they are still reflective of the experimental cross-section features in the near-threshold energy region.

The three-body break up reactions are less sensitive to details of the scattering matrix than the stripping reactions, as their phase space is larger and increases with increasing energy. That is why the peculiarities of the pairwise interactions in the three-body reactions are only noticeable in the threshold region. Our calculations of the $^{6}\mathrm{Li}(d,pt)^{4}\mathrm{He}$ and $^{6}\mathrm{Li}(d,n^{3}\mathrm{He})^{4}\mathrm{He}$ cross sections are in reasonable agreement with the experimental data in the energy region $E_d < 2$ MeV; above this energy region, the theoretical cross section significantly underestimates the experimental one. The specified underestimation may be attributed to the d-wave contributions of the cluster interactions, which were neglected in our calculations. For the d+^{7}Li system, only the experimental data for the $^{7}\mathrm{Li}(d,np)^{7}\mathrm{Be}$ reaction are available. Comparison with these data reveals agreement with the experimental value in the low-energy region $E_d < 10$ MeV and further underestimation of the cross section with increasing energy. The remaining calculations associated with the three-

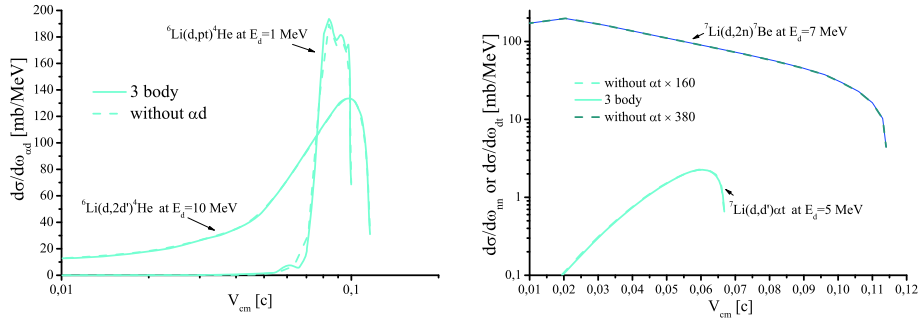

Fig. 11. (color online) Distributions, differentiated by the invariant mass, in the accurate calculation and in the calculation with neglected multiple interaction in the coupled pair of clusters versus relative rate in this pair (in speed of light unity). $\frac{d\sigma}{d\omega_{\alpha d}}$ for the ^{6}Li(d,2d')^{4}He at E_d=10 MeV and the ^{6}Li(d,pt)^{4}He at E_d=1 MeV on the left. $\frac{d\sigma}{d\omega_{nn}}$ for the ^{6}Li(d,2n')^{7}Be at E_d=7 MeV and $\frac{d\sigma}{d\omega_{dt}}$ for the ^{6}Li(d,d')αt at E_d=5 MeV.

body break up reaction and the radiation capture are presented in this paper for the first time.

Neglect of multiple scattering in (αd) and (αt) subsystems is equivalent to substitution in (21) $X_{13} \to Z_{13}$ and $X_{23} \to Z_{23}$. Figure 11 shows the differential by the invariant mass of (αd) cross section calculations of ^{6}Li(d,2d')^{4}He and ^{6}Li(d,pt)^{4}He reactions at E_d = 10 MeV and E_d = 1 MeV, respectively, versus the relative rate in the (αd) pair. Here, the dashed lines indicate calculations disregarding multiple (αd) scattering events. The obtained differential cross sections of the ^{7}Li(d,d't)^{4}He reactions at E_d = 5 MeV and the ^{7}Li(d,2n)^{7}Be at E_d = 7 MeV versus the relative rate within the clusters (dt) and (nn), respectively, are also presented in Fig. 11. Calculations neglecting multiple interactions in the (αt) subsystem are indicated by dashed lines and take into account multiplier 160 for the ^{7}Li(d,d't)^{4}He reaction and multiplier 380 for the ^{7}Li(d,2n)^{7}Be reaction. As can be seen, the role of multiple scattering in (αd) and (αt) subsystems turns out to be different. If we take the real lengths of deuteron elastic scattering on the ^{6}Li and ^{7}Li nuclei as a unit, the ratio of the scattering length calculated neglecting multiple scattering events in the (αd) and (αt) subsystems will be equal to 1.27 (or +27%) and 2.59 (or +159%), respectively, which is also in correlation with the results in Fig. 11. We believe that such divergence in properties in d+^{6}Li and d+^{7}Li systems depending on the interactions in the coupled (αd) and (αt) clusters within the adopted cluster scheme (3) reveals the significant role of inelastic dt interactions in the area surrounding the nucleus. This may be verified in the experimental investigation of dt systems or in forthcoming theoretical calculations of the partial phase shifts of dt elastic scattering.

V. CONCLUSION

The cross sections of most nuclear reactions in d + ^{6}Li and d + ^{7}Li systems existing in the energy range E_d = 0.5 – 20 MeV are presented in this work. The cross sections for radiation capture and some reactions with the (n+p+^{6}Li, 2d'+α, 2α+n, n+p+^{7}Li, α+d+t) three-body break up have been calculated for the first time. In general, the adopted parametrization provides an adequate characterization of the cross sections in the near-threshold energy range, and in some cases, specifically in the 2n + ^{7}Be channel, it is even possible to describe the experimental data up to 10 MeV. Despite the cluster behavior of both ^{6}Li and ^{7}Li nuclei, which is characterized by remarkable isolation of the cluster configurations, interaction in the coupled pair reveals itself in different ways for d + ^{6}Li and d + ^{7}Li. The next step in searching for d+Li stripping processes should carefully take into account the three-body nature of residual ^{7}Li, ^{8}Li, ^{7}Li, and ^{8}Be nuclei. Further studies are also possible in this area with the help of the d-wave interactions in the cluster subsystems and by employing some other kind of parametrization for elastic dt interactions.

References

[1] R. L. Macklin and H. E. Banta, Phys. Rev. **97**, 753-757 (1955)
[2] Ch. R. McClenahan and R. E. Segel, Phys. Rev. C, 370-382 (1975)
[3] A. J. Elwyn *et al.* (Argonne National Laboratory), Phys. Rev. C **16**, 1744-1756 (1977)
[4] R. Risler, W. Grüebler, A. A. Debenham *et al.*, Nucl. Phys. A **286**, 115-130 (1977)
[5] R. G. Clark, H. Hora, P. S. Ray *et al.*, Phys. Rev. C **18**, 1127-1132 (1978)
[6] Z. T. Bödy, J. Szabó, and M. Várnagy, Nucl. Phys. A **330**, 495-500 (1979)
[7] B. Y. Guzhovskij, S. Abramovich, A. Zvenigorodski *et al.*, Seriya Fizicheskaya **44**, 1983 (1980)
[8] L. N. Generalov, S. N. Abramovich, and S. M. Selyankina, Bulletin of the Russian Academy of Science: Physics **81**,

644-657 (2017)
[9] J. B. Woods and D. H. Wilkinson, Nucl. Phys. **61**, 661-674 (1965)
[10] A. E. Schilling, N. F. Mangelson, K. K. Nielson *et al*., Nucl. Phys. A **263**, 389-396 (1976)
[11] R. E. Holland, A. J. Elwyn, C. N. Davids *et al*., Phys. Rev. C **19**, 592-600 (1979)
[12] M. Avrigeanu, W. von Oertzen, U. Fischer *et al*., Nucl. Phys. A **759**, 327-341 (2005)
[13] T. Ye and Y. Watanabe, Phys. Rev. C **78**, 024611 (2008)
[14] T. Ye, Y. Watanabe, and K. Ogata, Phys. Rev. C **80**, 014604(1-8) (2009)
[15] J. L. C. Ford, Phys. Rev. B **136**, 953-960 (1964)
[16] D. L. Powell, G. M. Crawley, B. V. N. Rao *et al*., Nucl. Phys. A **147**, 65-80 (1970)
[17] M. V. Egorov, Nucl. Phys. A **986**, 175-194 (2019)
[18] F. S. Chwieroth, Y. C. Tang, and D. R. Thompson, Nucl. Phys. A **189**, 1-19 (1972)
[19] P. A. Schmelzbach, W. Crübler, V. König *et al*., Nucl. Phys. A **184**, 193-213 (1972)
[20] D. K. McDaniels, M. Drosg, J. C. Hopkins *et al*., Phys. Rev. C **7**, 882-888 (1973)
[21] M. Ivanovich, P. G. Young, and G. G. Ohlsen, Nucl. Phys. A **110**, 441-462 (1968)
[22] G. Audi, F. G. Kondev, M. Wang *et al*., The *Nubase2016* evaluation of nuclear properties, Chinese Physics C 41 (2017) 030001(1-138)
[23] H. Zankel, W. Plessas, and J. Haidenbauer, Phys. Rev. C **28**, 538-541 (1983)
[24] S. N. Abramovich, B. Ja. Guzhovskij, A. G. Zvenigorodskij *et al*., Bulletin of the Russian Academy of Science: Physics **50**, 62 (1986)
[25] J. M. Eisenberg and W. Greiner, *Excitation mechanisms of the nucleus electromagnetic and weak interactions*, (North-Holland Publ. Comp. Amsterdam-London), 1970